REPORT DOCUMENTATION PAGE

AD-A227 641

1. Agency Use Only *(Leave blank)*.	2. Report Date.	3. Report Type and Dates Covered.
	1990	Proceedings

4. Title and Subtitle.
The Fabric of a Consolidating Clayey Sediment Column, ODP Site 697

5. Funding Numbers.
Program Element No. 61153N
Project No 03205
Task No 330
Accession No DN257003

6. Author(s).
W. R. Bryant, R. H. Bennett, P. J. Burkett, and F. R. Rack

7. Performing Organization Name(s) and Address(es).
Naval Oceanographic and Atmospheric Research Laboratory*
Stennis Space Center, MS 39529-5004

8. Performing Organization Report Number.
PR 89:062:360

9. Sponsoring/Monitoring Agency Name(s) and Address(es).
Naval Oceanographic and Atmospheric Research Laboratory*
Ocean Sciences Directorate
Stennis Space Center, MS 39529-5004

10. Sponsoring/Monitoring Agency Report Number.
PR 89:062:360

11. Supplementary Notes.
*Formerly Naval Ocean Research and Development Activity
Proceedings of the Ocean Drilling Program

12a. Distribution/Availability Statement.
Approved for public release; distribution is unlimited.

12b. Distribution Code.

13. Abstract *(Maximum 200 words)*.

Consolidation of sediment is the main cause of porosity reduction with depth in the upper 1000 m of the sediment column. The consolidation of high-porosity sediment is mostly mechanical: the weight of the overlying sediment drives the rearrangement of individual particles and groups of sedimentary particles and domains. the mechanics of particle reorientation may be understood best through an examination of the sediment microfabric. A clay-rich sediment section 318 m thick, recovered during ODP Leg 113 from the South Orkney Microcontinental Margin, Site 697 in the Weddell Sea, was examined by transmission electron microscopy of ultrathin Sections. Reorientation of randomly arranged particles of this fine-grained, high-porosity (70%-75%) sediment occurs very gradually: porosity decreases to only about 50% at a depth of 318 m, because of the very fine-grained nature of the sediment and the presence of extremely fine-grained smectite, which imparts a very low permeability even at porosities of 50%.

14. Subject Terms.	15. Number of Pages.
(U) Sediment Transport; (U) Sediments; (U) Pore Pressure; (U) Clay	14
	16. Price Code.

17. Security Classification of Report.	18. Security Classification of This Page.	19. Security Classification of Abstract.	20. Limitation of Abstract.
Unclassified	Unclassified	Unclassified	SAR

Barker, P. F., Kennett, J. P., et al., 1990
Proceedings of the Ocean Drilling Program, Scientific Results, Vol. 113

18. THE FABRIC OF A CONSOLIDATING CLAYEY SEDIMENT COLUMN, ODP SITE 697[1]

W. R. Bryant,[2] R. H. Bennett,[3] P. J. Burkett,[3] and F. R. Rack[2]

ABSTRACT

Consolidation of sediment is the main cause of porosity reduction with depth in the upper 1000 m of the sediment column. The consolidation of high-porosity sediment is mostly mechanical: the weight of the overlying sediment drives the rearrangement of individual particles and groups of sedimentary particles and domains. The mechanics of particle reorientation may be understood best through an examination of the sediment microfabric. A clay-rich sediment section 318 m thick, recovered during ODP Leg 113 from the South Orkney Microcontinental Margin, Site 697 in the Weddell Sea, was examined by transmission electron microscopy of ultrathin sections. Reorientation of randomly arranged particles of this fine-grained, high-porosity (70%–75%) sediment occurs very gradually: porosity decreases to only about 50% at a depth of 318 m, because of the very fine-grained nature of the sediment and the presence of extremely fine-grained smectite, which imparts a very low permeability even at porosities of 50%.

INTRODUCTION

Two fundamental properties of a clayey sediment, the fabric and physico-chemistry, termed the microstructure, strongly influence and largely control the physical and mechanical properties of a sediment, including its consolidation behavior. An insight into the nature and behavior under stress of the silt-size particles and clay-size aggregates or domains (integral elements of the microstructure) that exist in the sediments at Site 697 can be studied using techniques of electron microscopy (EM). The clay minerals and larger sized particles in most sedimentary deposits are not of the same size, shape, and mineralogy; these characteristics, which are intimately coupled to the microstructure, play a significant role in establishing the ultimate fabric and sediment properties at the time of deposition and throughout the history of the deposit (Bennett et al., 1977). An understanding of clay microstructure and the methods of analysis are important because the results and interpretations have far-reaching effects on the fundamental conclusions and ideas of the basic origin, nature, and sources of sediment components. The understanding of clay microstructure is an important prerequisite to an understanding of the physical behavior of sedimentary deposits in response to static and dynamic loads and to variations in environmental conditions (Lambe, 1958a; Bennett et al., 1977).

The porosity reduction of sediments occupying the upper 1000 m of a sediment column is primarily the result of consolidation. Figure 1 illustrates the porosity profile for Hole 697B. Porosity decreases downhole at 0.051%/m. The loss of porosity and change in fabric with depth of burial govern many of the physical properties. Bulk density, shear strength, and acoustic velocity increase as water content (porosity) decreases. Gravitational loading forces individual sediment particles into new orientations with a reduction in pore space and expulsion of intervoid fluids. Other diagenetic processes such as cementation, recrystallization, and pressure point solution are other important factors of porosity reduction at greater burial depths.

Lower porosity also may result from the addition of sand to fine-grain sediment. An example of this is illustrated in Figure 1, where a 25% reduction in porosity occurs at the 13–15 mbsf level. The addition of clay to a diatomaceous sediment, which has very high porosity due to the high intravoid porosity of the diatom tests, brings about a large decrease in porosity.

At burial depths greater than 1000 m, the mechanical loading, cementation, and recrystallization processes appear inadequate as an explanation for porosity loss and fluid expulsion in these clayey sediments. Studies by Hinch (1980) suggest that the process controlling porosity reduction in shales may be thermophysical as well as mechanical. This involves thermodesorption of the structured water as temperature increases with depth of burial. Since reduction in porosity in the upper 1000 mbsf of sediment is mostly mechanical, a knowledge of the microstructure of a consolidating sediment mass will shed light on the mechanics of the consolidation process.

The purpose of this study is to (1) characterize the microstructure of a slowly consolidating clayey sediment mass as it compacts from a mud to a mudstone and (2) evaluate the relationship of sediment pore size, microfabric, and mineralogy to the porosity and the permeability of the material.

BACKGROUND

Physico-Chemistry of Clays

The physico-chemistry of clays is critical in determining the clay fabric of a marine deposit, especially in the early stage of formation (particles in suspension and at the depositional interface). Detailed studies of clay microstructure and its influence on the physical properties of sediment have been presented by Winterkorn (1948), Bolt (1956), Lambe (1958a), Rosenquist (1959, 1962), Warner (1964), Buchanan (1964), and Ingles (1968). Discussions and studies concerning the physico-chemistry of clays and colloids are found in Kruyt (1952) and van Olphen (1963).

The physico-chemical forces controlling clay mineral structure and the initial framework of clay fabric are essentially electrical in character. Suspended clay particles interact in response to the electrical nature of the particle surface and to the electrochemical characteristics of the surrounding aqueous medium. The important electrical forces are classified as primary valence bonds, hydrogen bonds, van der Waals forces, and simple electrostatic interactions (Lambe, 1958b). The phyllosilicate clay minerals are composed of sheets (tetrahedral and octahedral coordi-

[1] Barker, P. F., Kennett, J. P., et al., 1990. *Proc. ODP, Sci. Results*, 113: College Station, TX (Ocean Drilling Program).

[2] Department of Oceanography, Texas A&M University, College Station, TX 77843.

[3] Seafloor Geosciences Division, Naval Ocean Research and Development Activity, Stennis Space Center, MS 39529.

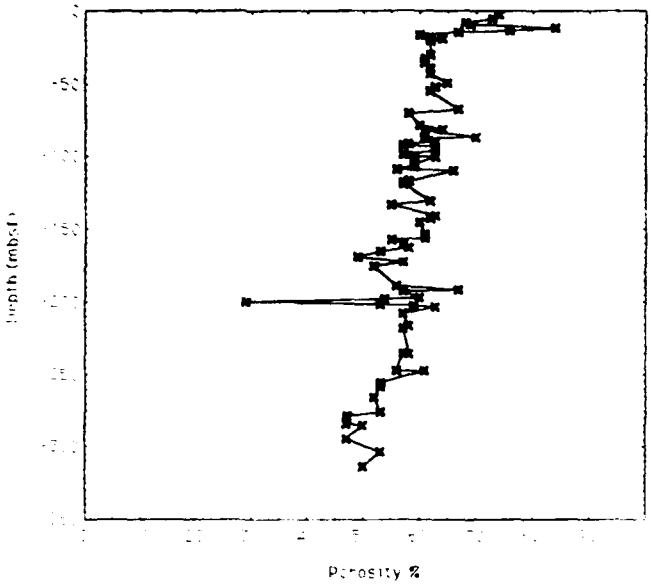

Figure 1. Laboratory porosity vs. depth profile for Hole 697A.

nation polyhedra) generally in 1-to-1 or 1-to-2 layers, such as one tetrahedral sheet plus one octahecral sheet (smectite, illite, and chlorite). This imparts a platy or sheet-like characteristic to many clay minerals, and for practical purposes they can be considered as being two-dimensional. Most clay particles are colloids, which range in size from about 1 μm to as small as 0.001 μm; however, some clay minerals are larger. In some cases, van der Waals forces and hydrogen bonds hold the two-dimensional clay mineral layers together to form relatively thin particles. During flocculation of suspended clay particles, deposition, and low-pressure diagenesis, clay crystals are not generally broken, nor are the clay layers separated (Lambe, 1958a). The breaking of interlayer bonds appears to indicate the onset of high-pressure diagenesis as revealed through studies of consolidated kaolinite (Cabrera and Smalley, 1971).

Electrostatic forces involve attraction between oppositely charged entities and repulsion between similarly charged ones. Electrostatic interactions are critical in determining clay microstructure, particularly clay fabric, because clay particles carry a net negative charge that is large compared to the particle mass and the net charge varies with the clay mineral type. The small positive charge carried by particle edges under certain conditions complicates physico-chemical interaction (Van Olphen, 1963; Bennett et al., 1977; Yariv and Cross, 1979; Bennett and Hulbert, 1986; Bryant and Bennett, 1988).

Early studies of clay fabric (Terzaghi, 1925; Goldschmidt, 1926; Casagrande, 1932; Lambe, 1953, 1958b) were followed by clay fabric studies employing X-ray and high-resolution electron microscopy techniques which depicted the actual arrangements and orientation of clay particles. The importance of fabric in determining the physical properties of sediments has been firmly established (Mitchell and Houston, 1969; Houston and Mitchell, 1969; Torrance, 1970). Bonding and effective stress and strength of soil have been studied by Mitchell et al. (1969), Anderson and Douglas (1970), Mitchell et al. (1971), and Singh (1970). Olson and Mesri (1970) discussed the influences of both the mechanical and physico-chemical mechanisms important in the compressibility of clays. Bryant and Bennett (1988) examined the fabric of Pacific Ocean red clays and revealed that one of the basic components of red clays is eolian shale clasts. Their paper is a good example of the use of fabric to solve a geological problem.

A few typical fabric types have been classified as honeycomb (Terzaghi, 1925; Casagrande, 1932), cardhouse (Goldschmidt, 1926; Lambe, 1953), turbostratic (Aylmore and Quirk, 1960), bookhouse (Sloane and Kell, 1966), and stairstep (O'Brien, 1971). Recently studies have revealed that the single plate concepts of fabrics are not wholly tenable and that the multiple unit, domain-type fabric is the rule for most sediments (Bennett, 1976; Bennett et al., 1981; Bennett and Hulbert, 1986).

Variations in particle size, shape, and composition, coupled with the depositional environment, physico-chemistry, transport mechanisms and energies, and changing environmental conditions, all increase the complexity of the sediment fabric for a particular sedimentary deposit. Only a few studies of the fabric of natural sedimentary material have been made; however, numerous studies (Lambe, 1958a, 1958b; Rosenquist, 1959) have dealt with the fabric and engineering behavior of laboratory-prepared material. Qualitative and ultimately quantitative studies of sediment fabric and microstructure of naturally occurring sediments are leading to reliable predictive capabilities of the physical behavior of clay sediments, a clearer understanding of the geotechnical properties, and a much better understanding of complex sedimentological processes.

MICROFABRIC TECHNIQUES

Critical Point Drying

Critical point drying is necessary to maintain the particle-to-particle integrity and quality of a clay sample to be examined by electron microscopy (Bennett et al., 1977; Tovey and Wong, 1978; Chiou, 1981). The critical point technique is a significant improvement over other dehydration methods because surface tension forces are avoided. At the critical temperature and pressure of a liquid no boundary exists between the liquid and the gas phase, and when the temperature is held above the critical point, the gas may be released until atmospheric pressure is reached. Thus the sample can be dried without surface tension effects.

Techniques Employed for the Examination of Microstructure

The series of techniques developed by Bennett (1976) for preparation of the clay samples for transmission electron microscope (TEM) fabric studies is as follows:

1. Subsampling of sediment from undisturbed core samples.
2. Replacement of saline interstitial water by a series of miscible fluids (ethyl alcohol-amyl acetate). Complete removal of interstitial water checked by the silver nitrate test (precipitation of silver chloride).
3. Careful wrapping of small specimens in thin lens paper and soaking of lens paper and specimen in amyl acetate.
4. Placement of wrapped specimens into the critical point chamber, purging of the specimen with liquid CO_2 replacing amyl acetate.
5. Critical point drying with CO_2.
6. Placement of dried, wrapped specimens into small individual desiccators and embedding of individual specimens under vacuum with a very low viscosity epoxy resin (SPURR).
7. Removal of specimens from the vacuum and subsequent curing of the epoxy resin at 60°-70°C.
8. Trimming of the specimens with glass knives prior to ultrathin sectioning. Larger specimens were trimmed with a jeweler's saw prior to trimming with a glass knife.
9. Ultrathin sectioning with a diamond knife (sections approximately 5×10^{-8} to 1×10^{-7} m thick (500–1000 Å) on a microtome.

10. Placement of ultrathin sections on copper grids, then very light carbon "sputtering" of ultrathin sections on grids in a vacuum evaporator.

SPURR epoxy resin is used for embedding because of its very low viscosity (60 cps) compared with ordinary epoxies (approximately 2000 cps). The usefulness and advantages of this epoxy have been determined by experiments on various Mississippi Delta and DSDP samples (Bennett et al., 1977). Submarine sediment samples with a high water content (low cohesive strength) remained intact if embedded while under a vacuum, but similar samples were found to collapse completely if they were impregnated at ambient pressure. Samples having a very complex fabric were found to retain their particle-to-particle structural integrity (Bennett et al., 1977). The impregnating techniques during this study were similar to those described by Brewer (1964) for impregnating soil samples under a vacuum.

THE NATURE OF SITE 697 SEDIMENTS

Site 697, located southeast of the South Orkney Islands in the northern Weddell Sea, was cored to a depth of 322.9 mbsf. The sediment sequence was mainly of hemipelagic origin, with a small siliceous biogenic component and numerous thin altered ash layers. Ice-rafted detritus was abundant near the base of the sequence. Two lithologic units were recognized (Barker, Kennett, et al., 1988), the upper one being divided into three subunits:

Unit I

Subunit IA: 0-15.5 mbsf—late Pleistocene age

Subunit IA is silty clay and diatom-bearing silty clay containing abundant illite, a common amount of chlorite, rare to abundant smectite, and rare to common amounts of kaolinite. Minor bioturbation is present.

Subunit IB: 15.5-85.7 mbsf—late Pleistocene age

Subunit IB consisted of clayey mud and clay with diatoms present in rare amounts or absent. Faint to moderate bioturbation is present. The upper 15 m of this subunit has a clay mineralogy similar to that of subunit IA. The remaining portion of the sediment contains abundant illite, common to abundant chlorite, rare to common kaolinite, and common amounts of smectite.

Subunit IC: 85.7-293.0 mbsf—Pliocene age

Subunit IC consists mainly of diatom-bearing clayey mud with clayey mud near the top, diatom clayey mud around 150 mbsf, and clay toward the base. Diatoms comprise 10%-30% of the sediment mass.

Unit II: 293.0-322.9 mbsf; Pliocene age

Unit II consists of silty muds and clayey muds with "weathered minerals" and rock fragments. The sediment is transitional between mud and mudstone. Minor bioturbation is present. The clay mineralogy of this subunit is similar to that of Subunit IC.

No calcium carbonate was present because Site 697 was below the CCD.

MICROFABRIC ANALYSIS OF SEDIMENT FROM SITE 697

Microfabric analysis was performed on samples from the following core positions:

Core 697A	Depth mbsf
1H-02, 61-63 cm	2.11
2H-02, 55-57 cm	7.35
3H-06, 55-57 cm	45.15
7H-01, 57-58 cm	76.57
10H-02, 52-54 cm	106.72
21X-02, 54-56 cm	207.94
27X-02, 54-56 cm	265.94
32X-04, 54-56 cm	317.24
32X-05, 54-56 cm	318.74

Core 697B	Depth mbsf

The sediments sampled by the use of the hydraulic piston corer (H) were of excellent quality and little disturbed. The sediments recovered by the extended core barrel (XCB) were highly disturbed and in most cases consisted of drilling "biscuits." The XCB samples used for the microfabric study were recovered from the least disturbed "biscuited" material. Undisturbed sections of lithified mudstone were recovered by the XCB at greater depths in the hole. In all cases samples recovered for microfabric analysis were taken from the high-quality least-disturbed section of the cores.

Figure 2 (Sample 1H-02) illustrates the basic microfabric of the high-porosity silty clays in the upper portion of the drill hole. The most prominent features of the section in Figure 2 are the silt-size holes. These holes were created by the fracturing and removal of silt-size illite shale clasts during the microtoming (ultrathin sectioning) process. The voids were filled with small fractured particles of highly compacted illite, some of which are arranged around the circumference of the holes. Similar features have been described by Bryant and Bennett (1988), who named these sectioning artifacts "fractillites," denoting a fractured illite-rich shale or argillaceous clast. They determined that these sediment particles were eolian in nature and were the main

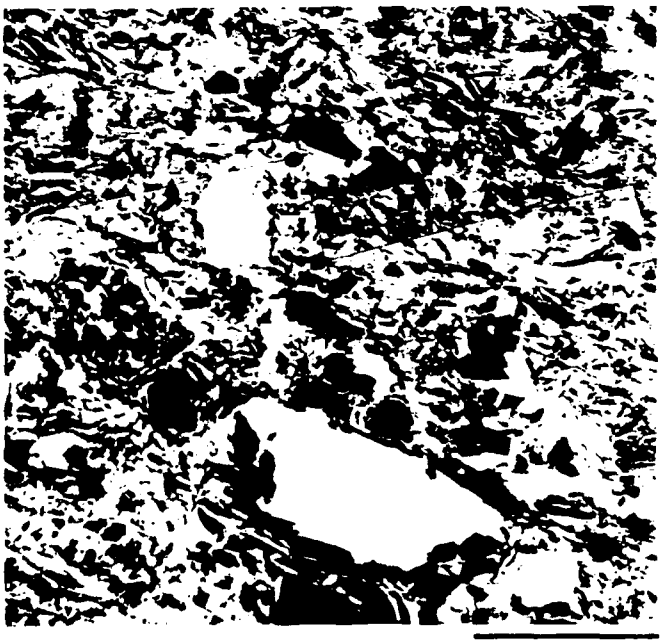

Figure 2. Clay fabric of transmission electron microscope (TEM) photomicrographic mosaic illustrating the nature of the microfabric of Hole 697A sediment at 2.11 mbsf. Large white areas are voids created by removal of large particles during the microtoming process. Scale bar = 10 μm.

constituent of the Pleistocene red clays of the North Pacific Ocean. Fractillites have the following characteristics:

1. They are brittle and fracture upon bending during the ultrathin sectioning process.
2. They are composed of 2:1 layer illite, as determined by selected area diffraction patterns on ultra-thin section.
3. The whole clasts are well rounded.
4. They are silt to clay sized.
5. They are associated with eolian quartz.
6. They are electron-dense.

These are the characteristics of the larger particles illustrated in Figure 2. These illite shale clasts may have been transported by winds from the Antarctic Peninsula, South America, or Australia.

Sediment at 2.11 mbsf has a porosity of 65%–70%, and the fabric is a random arrangement of clay particles and silt-size shale clasts. The silt-sized particles are held together by fine-grained smectite and chlorite (Fig. 2). The smectite is the binding material that gives support to the larger illite clasts, detrital illite, kaolinite, and quartz particles. The fleecy looking material is amorphous "smectite." Figure 3A shows a similar fabric in a sample from 7.35 mbsf. Figure 3B, an enlargement of portions of the mosaic shown in Figure 3A, illustrates the alignment of large illite and kaolinite domains. In Figure 3C the sheet-like material in the upper right-hand corner of the figure is also smectite. The general appearance of the fleecy smectite suggests that it is authigenic. Sediments at this level are overconsolidated by classical definition; see Bryant and Bennett (1988) for a detailed discussion of this phenomenon. Permeability of the material is in the range of 1×10^{-4} cm/s to 1×10^{-5} cm/s. The microfabric of this sediment section is in the first stages of consolidation, where the microstructure has sufficient strength to resist the stresses of the small overburden load impressed upon it.

Figure 4 illustrates the microfabric of sediment from another area of the sample at 7.35 mbsf (Sample 2H-02). The fabric is somewhat denser than that of the sediment depicted in Figure 3. Small fractured sections of silt-size particles are still visible, as are portions of a diatom test (right-hand side). Smectite is more abundant than in Sample 1H-01 and appears as an amorphous gray material binding the larger grains together. No preferred orientation of the clay particles is apparent.

The silty clays of the sediment at a depth of 45.15 mbsf (Sample 3H-06) contain mostly illite, chlorite, accessory minerals, and about 10% quartz. Figure 5 shows the thin section of a diatom test and the associated clay matrix. The clay particles form a fairly dense aligned mass around the test, approximately 4–5 μm in thickness. The large void created by the thin-sectioned diatom test illustrates how diatoms create large intra-test porosity, which can significantly influence the basic porosity of the sediment. Up to the point of collapse of the tests due to high overburden stress, the intra-test porosity is not effective in the consolidation process. Smectite appears to be a minor constituent and may be X-ray amorphous. These sediments with a porosity of 62% are underconsolidated (determined by consolidation tests), and the clay particles do not have a preferred orientation. The vertical effective stress at this stage of fabric development was calculated to be 200 kPa based on wet bulk density measurements.

Sample 7H-01 was taken at a depth of 76.57 mbsf. The sediment at this level consists of an illite-rich clay with 22% quartz and 4% volcanic glass. Chlorite, smectite, and kaolinite are common. The porosity of these sediments is approximately 60% and the vertical effective stress 430 kPa. At low magnification Figure 6 illustrates poorly developed preferred orientation of the clay particles. Figure 7 illustrates the local parallelism developed by the larger well-defined illite and kaolinite particles. The fleecy amorphous nature of the authigenic smectite is also visible. Pores of these sediments measure in the range of 0.1 μm or less. This sediment is underconsolidated and has a permeability of 2×10^{-7} cm/s.

Sample 10H-02 was taken at a depth of 106.72 mbsf. The sediment at this level is a silty clay composed of illite, chlorite, kaolinite and smectite, and about 14% quartz. The clay is slightly more compacted (Fig. 8) than in the overlying sample. Well-developed domains of parallel layers of large clay particles are visible. The supporting clay matrix consists of the amorphous material thought to be authigenic smectite. Porosity of this sediment is 59%, similar to the porosity at the 76.57 mbsf level. The lack of change in porosity with depth suggests that the sediment is underconsolidated, a suggestion that is supported by the ratio of undrained shear strength to effective stress and by consolidation tests (see Bryant and Rack, this volume). Figure 9 illustrates the relatively dense appearance of the smectite in this section. Pores in this material are very small and the permeability is very low, 5×10^{-8} cm/s.

Sample 21X-02 was taken at a depth of 207.94 mbsf. The sediment in this section consists of lower Pliocene silty clay, with illite, chlorite, kaolinite, and quartz comprising the main components. Smectite was not identified by X-ray diffraction. The TEM photomicrograph (Fig. 10) of this sediment shows it to consist of random particles and domains of 1–2 μm size clay particles. A supporting matrix of amorphous "smectite" occurs in significant amounts. The TEM photomicrographs in Figures 10 and 11A, -B, -C illustrate in detail the highly porous nature of the sediment and random orientation of the major clay minerals in edge-to-face contact and short chains. All four photomicrographs are from the same core section. Porosity of this material was 56%. The effective stress level at this sample depth was calculated to be 1300 kPa. Slightly more compaction has taken place within the sediment than within sediment at the 106.72 mbsf level.

Sample 27X-02 was taken at depth of 265.94 mbsf. The lower Pliocene sediments of this sample contain silty clay with 5% quartz. Illite was the most abundant clay, with chlorite, kaolinite, and smectite being common. The porosity of the sediment was 52%, slightly lower than at the 207.94 mbsf level. The effective vertical stress at this level was calculated to be 1940 kPa. Figure 12 shows a slight increase in orientation of the clay fabric; however, Figure 13 shows the preponderance of highly random clay domains of illite and smectite. The pores of this material appear quite large relative to the size of the particles. Note the very fine-grained nature of the material.

Sample 32X-05 was taken at a depth of 318.74 mbsf. The sediment at this depth was lower Pliocene silty clay, predominantly illite and chlorite. Kaolinite and smectite were present in rare amounts, with 10% quartz and 10% accessory minerals. The porosity of the material was 50%, making this the most compacted mudstone observed in this study. The calculated vertical effective stress at this depth was 2100 kPa. Figure 14 shows the fabric to be a highly random and chaotic clay mass. The fabric at high magnification has virtually no preferred orientation. It is interesting that, even at this degree of compaction, the large clay domains are supported in a matrix of finer clay particles, consisting mostly of smectite, some of which are small enough to be X-ray amorphous. Lower magnification views of this microfabric in Figures 15 and 16 show individual clay domains and clay particles to be somewhat more oriented than in Figure 12 (207.94 mbsf). The permeability of this material is extremely low, 1×10^{-10} cm/s.

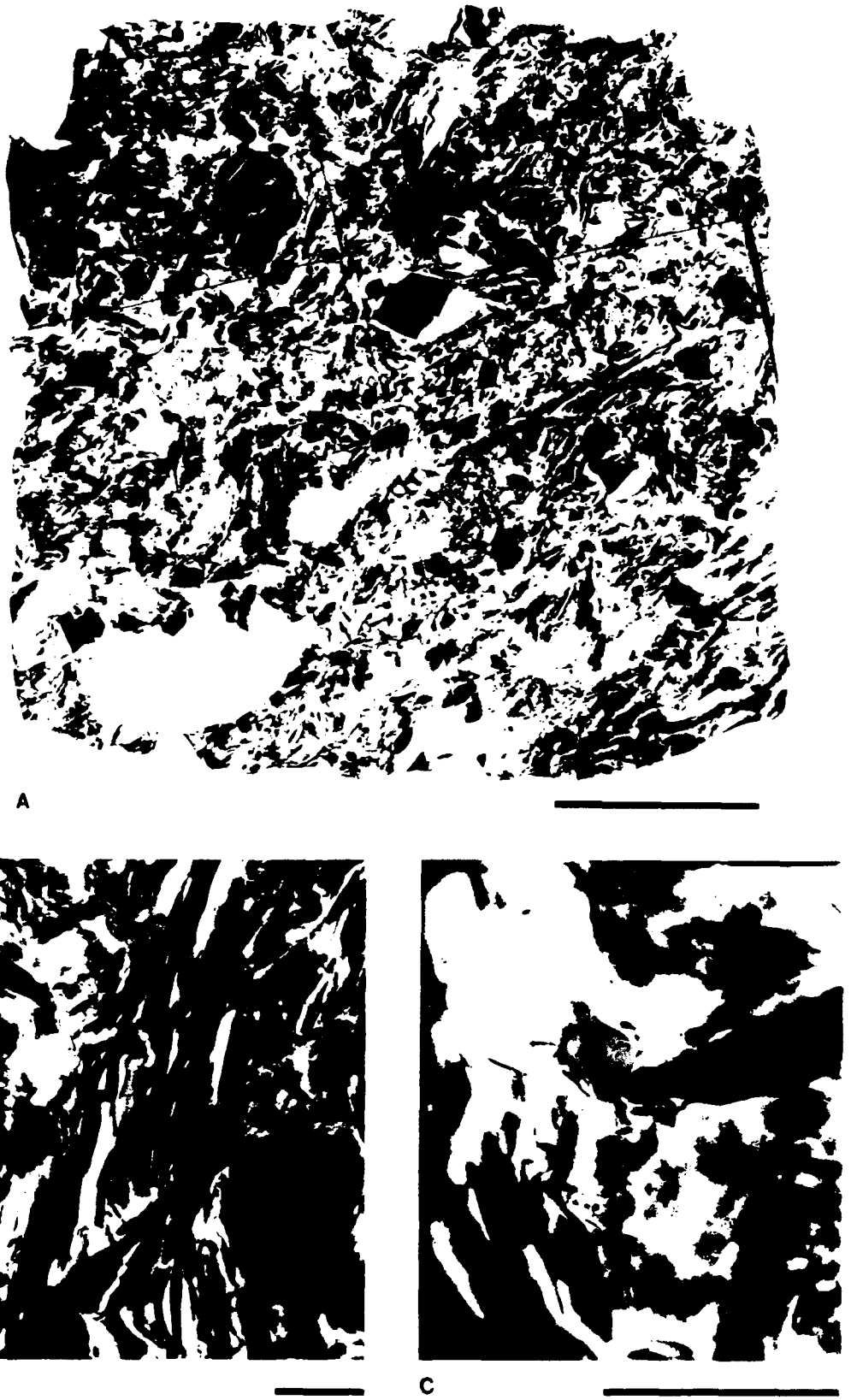

Figure 3. A. Mosaic of TEM photomicrographs of Sample 113-697A-2H-02, 55-57 cm, 7.35 mbsf. Note the very fine-grained matrix. Scale bar = 10 μm. B. TEM photomicrograph of enlarged section of A. Note the local areas of preferred particle orientation of domains. Scale bar = 2 μm. C. TEM photomicrograph of enlarged section of A. Note the high porosity. Scale bar = 1.0 μm.

Figure 4. Mosaic of TEM photomicrographs of Sample 113-697A-2H-02, 55–57 cm, 7.35 mbsf. Note the large diatom test and random orientation of particles. Scale bar = 10 μm.

SUMMARY AND CONCLUSIONS

TEM and SEM examination of the microfabric of the silty clayey sediments at Site 697 has illustrated the subtle changes in fabric as a clay mass consolidates from a mud to a mudstone. These observations confirm the suggested classic descriptions of clay fabric change and porosity reduction during the consolidation process. In contrast, Bennett et al. (1977) showed a stronger degree of preferred particle alignment for a consolidated sediment section of Mississippi Delta clays at depths of 150 mbsf. Significant consolidation and reorientation occurred, with a strong preferred particle orientation normal to the overburden stress. This occurred at effective stresses of $4–7 \times 10^2$ kPa because of the presence of an interbedded 25-m-thick drainage path (fine sand) overlying the compacted Pleistocene clays (Bennett et al., 1977, 1981).

Under low overburden stresses the fabric of a silty clay sediment appears as a random arrangement of clay particles, eolian shale clasts, diatoms, quartz particles, and clay domains. At this stage of compaction the material has a high porosity (74%) and a relatively high permeability (1×10^{-4} to 1×10^{-5} cm/s). With increasing depth of burial, increased mechanical forces in the form of overburden stress slowly reorient the clay particles. This in turn decreases porosity, expels intergranular pore fluids, decreases the permeability, and lengthens the compaction process. The drastic decrease in permeability (from 3 to 10 orders of magnitude faster than porosity: Bryant et al., 1986) imparts an underconsolidation characteristic to the sediment. This underconsolidation is common to many clayey marine sediments found in the deep ocean basins. We suggest that the onset of preferred fabric orientation of these sediments below a depth of 200 mbsf at this site produces an anisotropic material with respect to permeability and acoustic velocity.

A

B

Figure 5. Mosaic of TEM photomicrographs of Sample 113-697B-3H-06, 55–57 cm, taken at a depth of 45.15 mbsf. Note large void of diatom test (**A**) and arrangement of clay particles oriented parallel to surface of test (**A** and **B**). Scale bars = 10 and 5 μm.

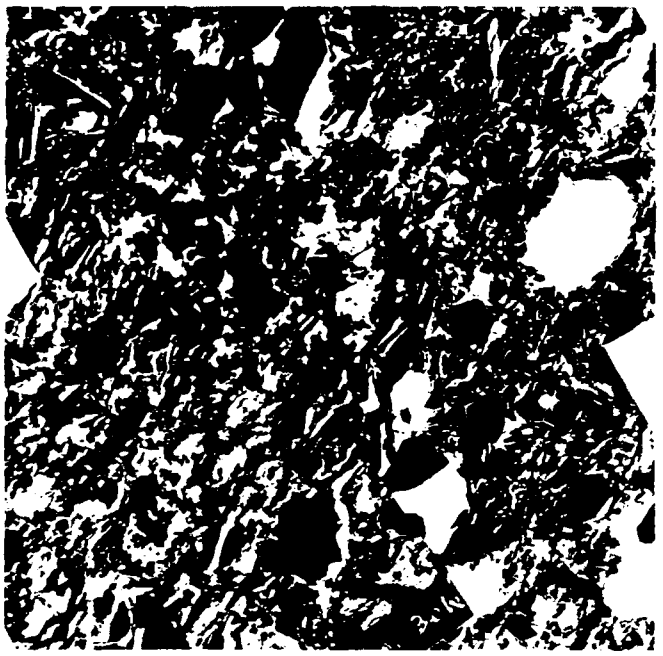

A

B

Figure 6. **A.** Mosaic of TEM photomicrographs of Sample 113-697B-7H-01, 57–58 cm, taken at a depth of 76.57 mbsf. Note the bimodal distribution of sediment particles and their random arrangement. The larger particles are supported by the "smectite" matrix. Scale bar = 10 μm. **B.** TEM photomicrograph. Note the predominantly random arrangement of clay particles and the increase in density. Scale bar = 5 μm.

Figure 7. TEM photomicrograph of enlarged section of Figure 6 illustrating the local parallelism of the illite and kaolinite particles. Note the very dense and fine-grained matrix. Sampled at 76.57 mbsf. Scale bar = 2 μm.

Figure 8. TEM photomicrograph of Sample 113-697B-10H-02, 52–54 cm, showing a compressed fabric of a silty clay containing chlorite, kaolinite, illite, and smectite. Sampled at 107.2 mbsf. Scale bar = 5 μm.

Figure 9. TEM photomicrograph enlargement of part of Figure 8, illustrating the dense nature of the smectite fabric. Note the fine-grained matrix between larger domains. Scale bar = 1 μm.

Figure 10. Mosaic of TEM photomicrographs of Sample 113-697B-21 X-02, 54-56 cm, from a depth of 207.94 mbsf. Particles are randomly oriented, but note the apparent particle orientation caused by the microtoming process: linear cuts (white) give a fictitious orientation. Scale bar = 10 μm.

The identification of fractured illite shale clasts ("fractillites") and associated quartz grains in the upper Pleistocene portions of Hole 697 indicates that these fractions of the sediment could be of an eolian origin.

ACKNOWLEDGMENTS

Practical support for this research was provided by USSAC of JOI. Thanks are extended to those reviewers whose efforts made this paper much better than the original draft.

REFERENCES

Anderson, O. B., and Douglas, A. G., 1970. Bonding, effective stresses, and strength of soils. *J. Soil Mech. Found. Div., Proc. Am. Soc. Civ. Eng.* 96:1073-1077.

Aylmore, L.A.G., and Quirk, J. P., 1960. Domain or turbostratic structure of clay. *Nature*, 187:1046-1048.

Barker, P. F., Kennett, J. P., et al., 1988. *Proc. ODP, Init. Repts.*, 113 College Station, TX (Ocean Drilling Program).

Bennett, R. H., 1976. Clay fabric and geotechnical properties of selected submarine sediment cores from the Mississippi Delta [Ph.D. dissert.]. Texas A&M Univ., College Station.

Bennett, R. H., Bryant, W. R., and Keller, G. H., 1977. Clay fabric and geotechnical properties of selected submarine sediment cores from the Mississippi Delta. *NOAA Prof. Pap.*, U.S. Dept. of Commerce, 9:1-86.

_____, 1981. Clay fabric of selected submarine sediments: fundamental properties and models. *J. Sed. Pet.*, 51:217-232.

Bennett, R. H., and Hulbert, M. H., 1986. *Clay Microstructure*. Boston (International Human Resources Development Corp.).

Bolt, G. H., 1956. Physico-chemical analysis of the compressibility of pure clays. *Geotechnique*, 6:86-93.

Brewer, R., 1964. *Fabric and mineral analysis of soils*. New York (John Wiley and Sons).

Bryant, W. R., Wetzel, A., Taylor, E., and Sweet, W., 1986. Consolidation characteristics and permeability of Mississippi Fan sediments. *In* Bouma, A. H., Coleman, J. M., Meyer, A. W., et al., *Init. Repts. DSDP*, 96: Washington (U.S. Govt. Printing Office), 797-809.

Bryant, W. R., and Bennett, R. H., 1988. Origin, physical, and mineralogical nature of red clays: the Pacific basin as a model. *Geo-Mar. Lett.*, 8:189-249.

Buchanan, P. N., 1964. Effect of temperature and absorbed water on permeability and consolidation characteristics of sodium and calcium montmorillonite [Ph.D. dissert.]. Texas A&M Univ., College Station.

Cabrera, J. G., and Smalley, L. J., 1971. Engineering behavior and structure of compacted clay, discussion and reply. *J. Soil Mech. Found. Div., Proc. Am. Soc. Civ. Eng.*, 19:802-803.

Casagrande, A., 1932. The structure of clay and its importance in foundation engineering. *Jour. Boston Soc. Civ. Eng.*, 19.

Chiou, W.-A., 1981. Clay fabric of gassy submarine sediments [Ph.D. dissert.]. Texas A&M Univ., College Station.

Goldschmidt, V. M., 1926. Undersokelser over lersedimenter. *Nordisk-jordbrugsforskuing*, 4-7:434-445.

Hinch, H. H., 1980. Nature of shales in expulsion, problems of petroleum migration. *In* Roberts, W., and Cordell, R. (Eds.), *AAPG Studies in Geology*, 10:1-18.

Houston, W. N., and Mitchell, J. K., 1969. Property interrelationships in sensitive clays. *J. Soil Mech. Found. Div., Proc. Am. Soc. Civ. Eng.*, 95:1037-1062.

Ingles, O. G., 1968. Soil chemistry relevant to the engineering behavior of soils. *In* Lee, L. K. (Ed.), *Soil Mechanics, Selected Topics*, London, (Butterworths), p. 1-57.

Kruyt, H. O. (Ed.), 1952. *Colloid Science, Irreversible Systems*. Amsterdam (Elsevier).

Lambe, T. W., 1953. The structure of inorganic soil. *Proc. Am. Soc. Civ. Eng.*, 79:1-49. (Separate 315).

_____, 1958a. The structure of compacted clay. *J. Soil Mech. Found. Div., Proc., Am. Soc. Civ. Eng.*, 84:1-35. (Separate 1654).

_____, 1958b. The engineering behavior of compacted clay. *J. Soil Mech. Found. Div., Proc., Am. Soc. Civ. Eng.*, 84:1-35. (Separate 1655).

Mitchell, J. K., and Houston, W. N., 1969. Causes of clay sensitivity. *Mech. Found. Div., Proc., Am. Soc. Civ. Eng.*, 95:845-871.

Mitchell, J. K., Singh, A., and Campanella, R. G., 1969. Bonding, effective stresses, and strength of soils. *J. Soil Mech. Found. Div., Proc. Am. Soc. Civ. Eng.*, 95:1219-1246

_____, 1971. Bonding, effective stresses, and strength of soils. *J. Soil Mech. Found. Div. Proc., Am. Soc. Civ. Eng.*, 97:478.

O'Brien, N. R., 1971. Fabric of kaolinite and illite floccules. *Clays and Clay Minerals*, 19:353-359.

Olson, R. E., and Mesri, G., 1970. Mechanisms controlling compressibility of clays. *J. Soil Mech. Found. Div., Proc., Am. Soc. Civ. Eng.*, 96:1863-1878.

Rosenquist, I. Th., 1959. Physico-chemical properties of soils: soil-water systems. *J. Soil Mech. Found. Div., Proc., Am. Soc. Civ. Eng.*, 85:31-53.

_____, 1962. The influence of physico-chemical factors upon the mechanical properties of clays. *Ninth National Conf. on Clays and Clay Minerals*, 9:12-27.

Singh, S., 1970. Bonding, effective stresses, and strengths of soils. *J. Soil Mech. Found. Div., Proc., Am. Soc. Civ. Eng.*, 96:1469-1473.

Sloane, R. L., and Kell, T. R., 1966. The fabric of mechanically compacted kaolinite. *Clays and Clay Minerals*, 14:289-296.

Terzaghi, K., 1925. Principles of soil mechanics settlement and consolidation of clay. *Eng. New-Record*, 874-878.

Torrance, K. J., 1970. Causes of clay sensitivity. *J. Soil Mech. Found. Div. Proc., Am. Soc. Civ. Eng.*, 96:360-361.

Tovey, N. K., and Wong, K. Y., 1978. Preparation, selection and interpretation problems in scanning electron microscope studies of sediments. *In* Whalley, W. B. (Ed.), *Scanning Electron Microscopy in the Study of Sediments*. Norwich, England, Geo-Abstracts, 181-199.

van Olphen, H., 1963. An analysis of the influence of the physical-chemical factors upon the consolidation of fine-grained clastic sediments [Ph.D. dissert.]. Univ. California, Berkeley.

Winterkorn, H. F., 1948. Physico-chemical properties of soils. *Proc. 2nd International Conf. Soil Mechanics Foundation Engineering*, Rotterdam, pp. 23-29.

Yariv, S., and Cross, H., 1979. *Geochemistry of colloid systems* (Springer-Verlag), Berlin.

Date of initial receipt: 1 March 1989
Date of acceptance: 16 October 1989
Ms 113B-174

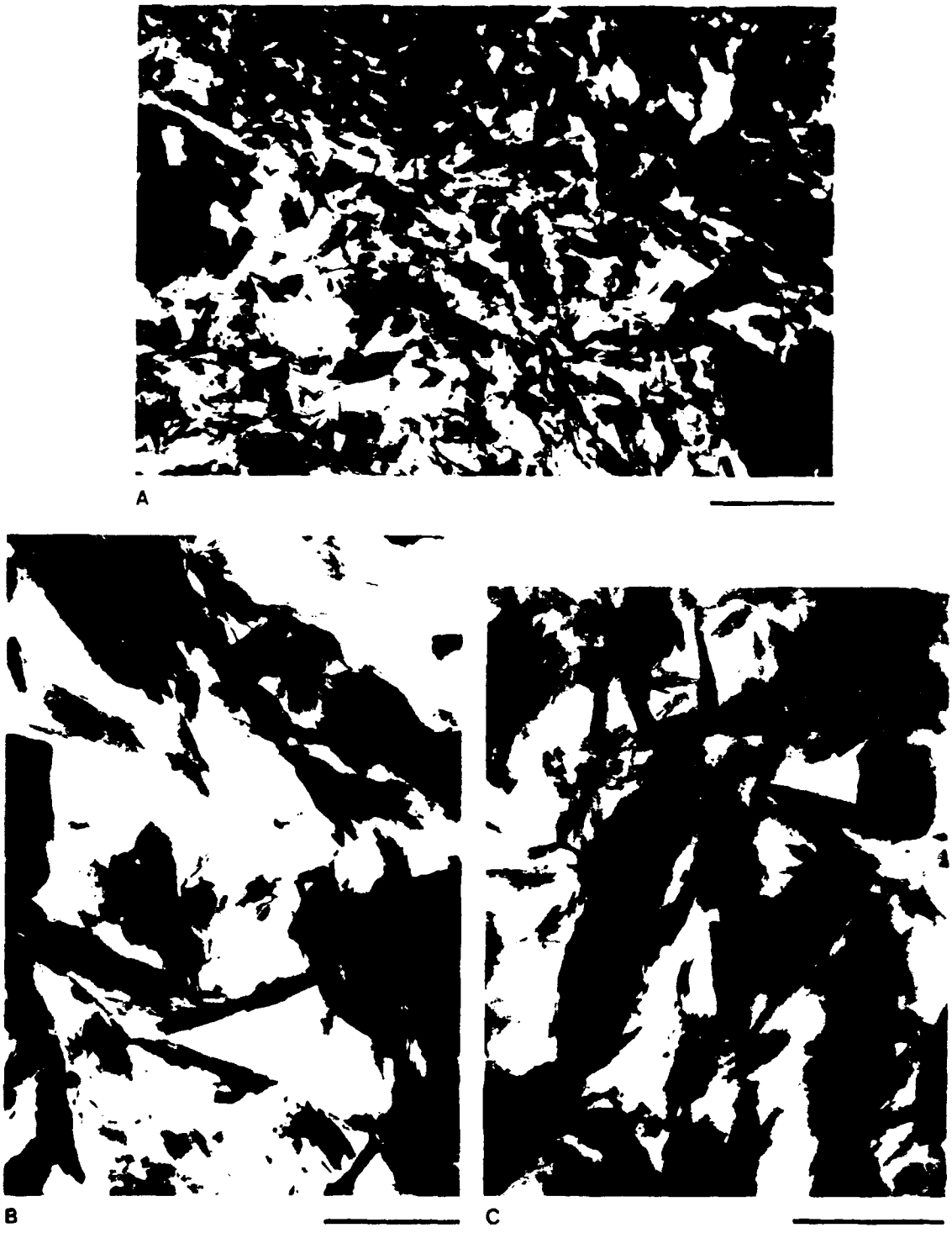

Figure 11. A. TEM photomicrograph of Sample 113-697B-21X-02, 54-56 cm, showing the high degree of randomness of the clay particles and domains. Porosity remains relatively high at 56%. Scale bar = 1 μm. B and C. High magnification of Sample 113-697B-21X-02, 54-56 cm, depicting the relatively high porosity and randomness of domains in short chains and in edge-to-face contact. Note the fleecy amorphous "smectite" that clusters around the electron-dense domains. Scale bar = 0.5 μm.

Figure 12. TEM photomicrographs of Sample 113-697B-27H-02, 54–56 cm, from a depth of 266.4 mbsf. Note the relatively high porosity and random orientation of particles. There is a slight preferred particle orientation. Scale bar = 2 μm.

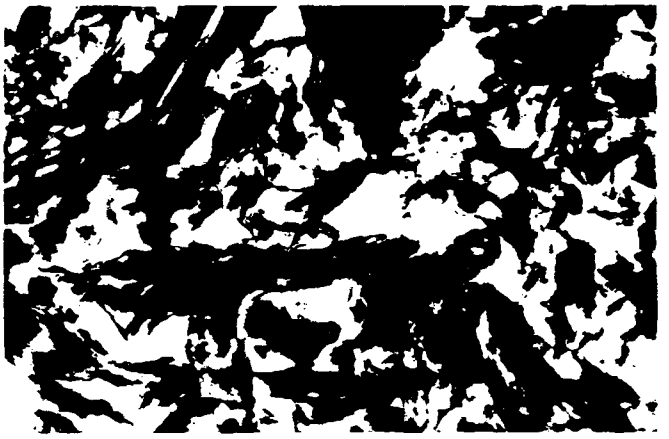

Figure 13. TEM photomicrograph of Sample 113-697B-27X-02, 54–56 cm, showing the highly random orientation of clay domains of illite and smectite. Note the "smectite" clusters around the electron-dense domains. Scale bar = 0.5 μm.

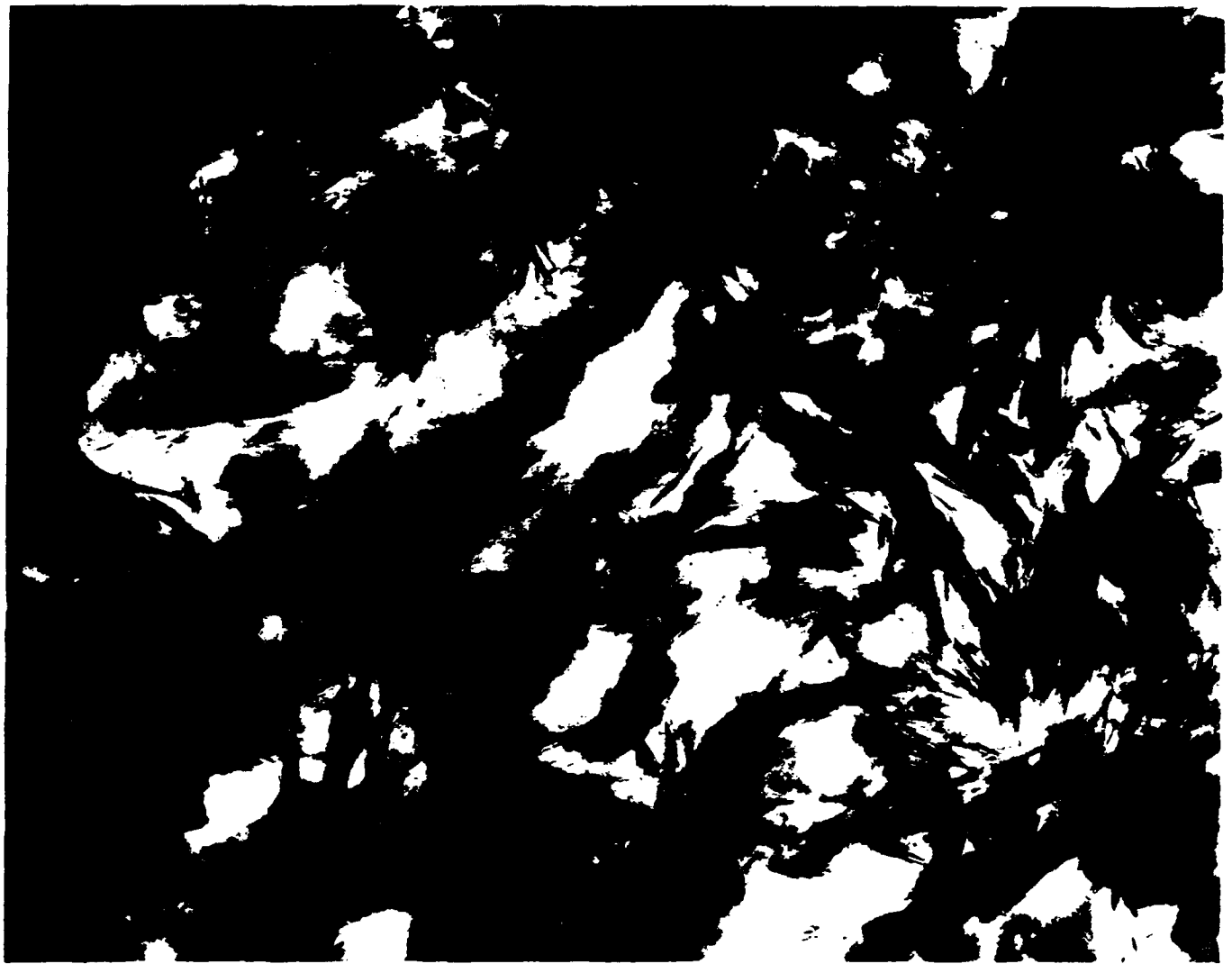

Figure 14. High-magnification TEM photomicrographs of Sample 113-697B-32X-04, 54–56 cm, from a depth of 317.24 mbsf. Local areas depict random orientation of numerous small particles. Scale bar = 0.25 μm.

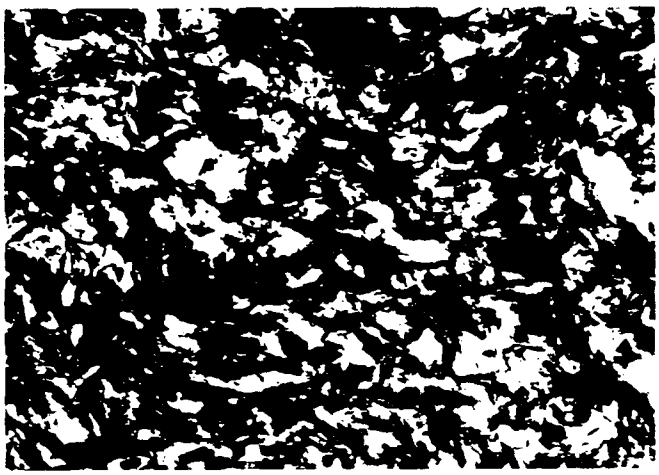

Figure 15. Sample 113-697B-32X-04, 54–56 cm. Note that, at lower magnification, numerous particles show some preferred orientation normal to the principal stress direction. Scale bar = 1 µm.

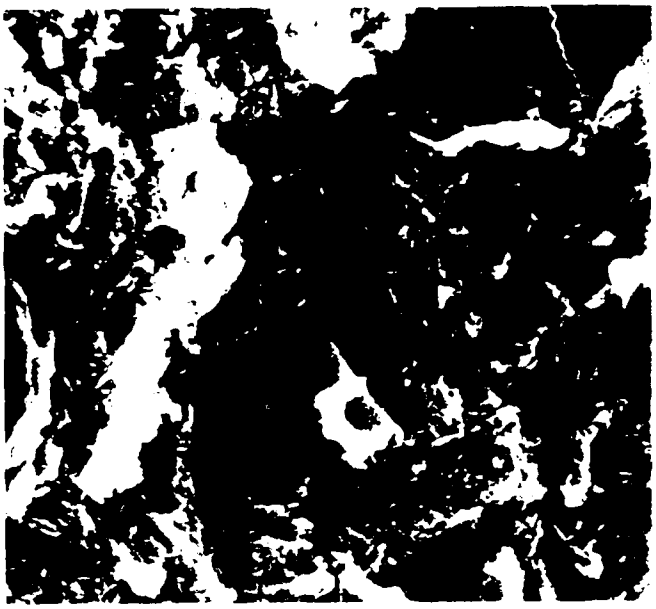

Figure 16. SEM photomicrograph of Sample 113-697B-32X-05, 54–56 cm, showing the oriented fabric of the moderately compressed sediment. Scale bar = 5 µm.